Paper No P1-38

Parallel expansion of density bursts

G. Chiavassa[a,*], H. Bufferand[a], G. Ciraolo[a], Ph. Ghendrih[b], H. Guillard[c], L. Isoardi[a], A. Paredes[a], F. Schwander[a], E. Serre[a], P. Tamain[b]

(a) M2P2 CNRS/Aix-Marseille Université/Ecole Centrale Marseille, Technopôle de Château Gombert, F-13451 Marseille, France, ANR ESPOIR,

(b) IRFM, CEA-Cadarache, F-13108 St. Paul-lez-Durance Cedex, France

(c) INRIA, BP. 93, 06902 Sophia Antipolis Cedex, France

Abstract

Evidence of poloidally localized cross-field transport in experiments and theoretical analysis of turbulence transport governs the onset of parallel transport towards equilibrium. When cross-field transport appears in bursts, both for ELM relaxation events and microturbulence, the parallel transport of particles is shown to generate fronts that propagate with supersonic velocities. It is shown that after a short transient the density structure is no longer monotonic and that the two fronts (one co, the other counter the magnetic field) are independent. Furthermore, the time trace of the particle flux at a given location is characterized by a sharp rise followed by a longer time scale relaxation. Comparing the time delay and magnitude of the density burst at two locations allows to estimate the magnitude and the location of the generation of the front.

JNM Keywords: M0200, T0100.

PSI-19 Keywords: Parallel Transport, Cross-Field Transport, ELM.

PACS: 52.65.Kj, 52.35.g,52.35.Mw, 52.35.Tc

Corresponding Author: G. Chiavassa, Ecole Centrale Marseille, Technopôle de Château Gombert, F-13451 Marseille, France. Email: *guillaume.chiavassa@centrale-marseille.fr*

Acknowledgments: This work has been supported by the ANR ESPOIR (ANR09-0035-01).

I. INTRODUCTION

The parallel expansion of a density burst was first addressed in the case of pellet injection since standard plasma operation was usually considered within the frame of nearly constant density on magnetic surfaces or along field lines. Furthermore, the standard analysis based on diffusive transport led to smooth temporal variations and structures in space. However, recent experimental and theoretical evidence have demonstrated that the edge and SOL plasma is characterized by strong transients, such as ELMs for MHD turbulence or so-called blobs for microturbulence. A common characteristic of these transient transport events is their ballooned nature that leads one to consider that the over-dense filaments that propagate with a ballistic radial velocity have in fact a finite parallel extent during the cross-field transport sequence [3, 5]. The filament structure that has been readily observed experimentally [4] would then stem from a second sequence governed by fast parallel transport that would tend to restore a homogeneous parallel structure characterized by a vanishing parallel wave vector.

The scope of this paper is to analyze the latter parallel transport sequence, in particular regarding particle transport. The key assumption of our approach is that the cross-field transport event leads to an overdense region with finite parallel extent. The parallel expansion of this density burst is then investigated in the framework of a 1-dimensional and isothermal model. Analytical calculations and numerical simulations allow one to describe the parallel expansion mechanisms. The model is described in Section 2 together with the expansion dynamics. In Section 3, we show how the comparison between the co and counter (with respect to the magnetic field direction) expansion events when recorded away from the mid-plane, provides a means to determine the location and magnitude of the cross-field transport event that has generated the expansion sequence. A summary and discussion conclude the paper in Section 4.

II. PARALLEL FRONT GENERATED BY A DENSITY BURST

The direction of interest aligned along the field line is labeled by the curvilinear abscissa s. The initial state of the density burst is described by a constant density n_b extending

over a scale $2 * s_b$ and separated from an uniform background plasma of density n_0 by a discontinuity at $s = \pm s_b$. At the initial time $t = 0$, both the background plasma and the burst will be considered at rest with vanishing velocity. To investigate the expansion of this over-density we consider the particle balance equation with no source as well as the balance equation of the total plasma momentum. In the isothermal framework, the sound velocity $c_s = \sqrt{(T_e + T_i)/m_i}$ allows one to normalize the velocity and therefore to consider the Mach number M. Similarly, one can introduce the parallel scale $2 * L_\parallel$ of the field line. The time scale is normalized to the parallel confinement time $\tau_\parallel = L_\parallel / c_s$. Since the system is homogeneous with respect to the density, one can normalize the density by any value, a possible choice being that of the background density n_0. The dimensionless equations then take the form:

$$\frac{\partial}{\partial t} N \; + \; \frac{\partial}{\partial z}\big(NM\big) = 0 \tag{1}$$

$$\frac{\partial}{\partial t}\big(NM\big) \; + \; \frac{\partial}{\partial z}\Big(N\big(1 + M^2\big)\Big) = 0. \tag{2}$$

In this set of equations N, z and t are respectively the normalized density, curvilinear abscissa and time. The initial conditions introduce two control parameters: the extent of the density burst z_b and the density of the burst $N_b = n_b/n_0$. In the present analysis, since one assumes $z_b \ll 1$, this parameter will not play a role. Note that this assumption is governed by the ballooned nature of cross-field transport while the filament structure will result from the fast expansion described below. It can be shown [1] that generically a rarefaction wave preceded by a front will bridge the background plasma to the initial state of the burst as sketched on figure 1. Two important regions are found, the front itself, namely the discontinuity between the density N_F and the background density $N_0 = 1$, and the rarefaction wave that exhibits an exponential density wave form, or equivalently a linear dependence when considering $Log(N)$, and a linear increase of M. The front velocity and density are determined by the following equations:

$$c_F - \frac{1}{c_F} + Log\big(c_F^2\big) \; = \; Log\big(N_b\big) \tag{3}$$

$$\sqrt{N_F/N_0} \; = \; c_F. \tag{4}$$

As readily noticeable in the above equation as well as on figure 2, the front velocity is larger than 1, hence supersonic. One can also show that the right end of the rarefaction wave also has a positive velocity $c_F - 1$, while the left hand side of the rarefaction wave

has a velocity -1. Therefore, this point rapidly shifts towards the symmetry point of the system set at $z = 0$ and this first phase of the expansion will last from $t = 0$ to $t = z_b$. After this transient, all the numerical simulations reveal the same behavior: the front part appears to expand in an unperturbed fashion until a triangular shape is reached for $Log(N)$ and M, see figure 3. Once such a structure is achieved, the density burst cannot further increase its length without decreasing the front density N_F and consequently its velocity c_F, Eq.(4). Within our present understanding, it is difficult to determine analytically when such a state is reached. For convenience, we introduce a reference state with a triangular shape for $Log(N)$ extending from $z = 0$ to $z = L_{F0}$, such that N_{F0} and c_{F0} are determined by the initial phase of the density expansion, Eqs.(3, 4). The extent of the front is then set by particle conservation: $\mathcal{N} = N_0(N_{F0}/N_0 - 1)L_{F0}(t_{F0})/Log(N_{F0}/N_0) = N_0(N_b/N_0 - 1)z_b$ where $L_{F0}(t_{F0}) = c_{F0}t_{F0}$. In this relation, t_{F0} is the characteristic time for the onset of the propagation of the triangular density pulse. It is important to stress that given the symmetry of the problem this time also corresponds to the separation of the initial density burst into two independent parts. In the following stage of the expansion, the triangular burst shifts and expands along the z-axis. The density of the front decreases, which governs in turn a decrease of the front velocity, Eq.(4). A similar evolution is described in [2] but requires to be modified to take into account that the triangular shape is considered for $Log(N)$, leading to the following relations:

$$t \leq t_{F0} \qquad N_F(t) = N_{F0} \tag{5}$$

$$t \geq t_{F0} \qquad \frac{N_F(t+\delta t)}{N_0} = \frac{N_F(t)}{N_0}\Big(1 + \frac{M_F(t)}{L_F(t)}\delta t\Big)^{-1} \tag{6}$$

where M_F is the Mach number at the front location. It is related to the front velocity c_F by the relation $M_F = c_F - 1/c_F$. The pulse extent $L_F(t)$ is obtained by considering the particle conservation described above. Using this relation, the time dependence of the front density is governed by:

$$\frac{dN_F}{dt} = -\frac{N_0^2}{\mathcal{N}}\frac{(N_F/N_0 - 1)^3}{Log(N_F/N_0)\sqrt{N_F/N_0}}. \tag{7}$$

Upon integration, one then finds that:

$$\Delta\tau = \mathcal{W}(N_F/N_0) = \tau - \Big(\tau_{F0} - \mathcal{W}(N_{F0}/N_0)\Big) \qquad \mathcal{W}(y) = \int_y^\infty dy \frac{Log(y)\sqrt{y}}{(y-1)^3}. \tag{8}$$

The normalized evolution time τ is defined as $\tau = t\,\mathcal{N}/N_0$. This allows one to compute the generic evolution of the front density, represented on figure 4. The initial time for the onset

of the triangular pulse propagation, τ_{F0}, can be expressed as a function of the front density, $\tau_{F0} = Log(N_F/N_0)/\big((N_F/N_0 - 1)\sqrt{N_F/N_0}\big)$. Modifying the particle content of the initial burst then only leads to a change of the ratio between the normalised time τ and time t. Given these relations, it is also possible to compute the location of the front position z_F:

$$\Delta Z_F = \mathcal{V}(N_F/N_0) = \frac{N_0}{\mathcal{N}}\big(z_F \; - \; \delta z_{F0}\big) \qquad \mathcal{V}(y) = \int_y^\infty dy \frac{Log(y)y}{(y-1)^3} \tag{9}$$

$$\delta z_{F0} \; = \; z_{F0} - \frac{\mathcal{N}}{N_0}\mathcal{V}(N_{F0}/N_0) \tag{10}$$

Taking into account Eq.(8), one can then determine the evolution of the front location, represented on figure 5. As expected, and according to the decrease of the front density, the position of the front asymptotically converges towards a sonic displacement. The other characteristic features of the triangular front such as the front extension L_F and the e-folding length λ_F (or slope of Log(N)) are:

$$L_F \; = \; Log(N_F/N_0)\lambda_F \qquad \lambda_F = \frac{\mathcal{N}}{N_0}\frac{1}{N_F/N_0 - 1}. \tag{11}$$

III. CHARACTERIZING THE CROSS-FIELD TRANSPORT EVENTS

The analytical expressions discussed in Section II are exact within the framework of triangular shaped pulses with no losses during the parallel expansion. It allows us to compare the signature of the two triangular pulses generated by the initial density burst. This provides information on the cross field transport in particular when the measurement points are located at different distances from the initial location of the burst $z \approx 0$. Possible experimental situations where it is possible to apply this approach are 1) the ion saturation current on a set of two Langmuir probes connected in both co and counter directions [3] as well as 2) the energy imprint of an ELM on the inner and outer target plates of the divertor. In this section, we analyze two time traces, corresponding to two different measurement points, figure 6, obtained by a numerical integration of Eqs.(2). Let us consider the traces of the correlated density bursts labeled 1, in the co-direction at probe location $z = z_1$, and 2, in the counter-direction at probe location $z = -z_2$, recorded at a large enough distance from the symmetry point, $z_1, z_2 \gg z_b$. The distance between the two measurement points along the parallel direction is: $\ell_{1,2} = z_1 + z_2$. It can be noted in the time trace that the data recorded at the measurement point 2 exhibits characteristic features of bursts recorded during ELMs or

microturbulence fluctuations. Data from measurement point 1 is very similar but exhibits a rather flat maximum. This indicates that z_1 is close enough from the location of the initial burst so that the final phase of the burst expansion, with triangular shape, has not been reached yet. The signal on either probe locations exhibits a sharp rise followed by an exponential decay, see figures 6-7. Within the front description, the features of the density rise is not described but is characterized in the simulation by the very small relaxation time $1/\gamma_{front}$, figure 7, where $\gamma_{front} = d_t(N/N_0)$. One can also observe a linear decrease of the relaxation time during the decay of the signal. This effect is readily expected since the pulse e-folding length decreases with the front density and therefore with time, Eq.(7). Let us determine on figure 6 the front density by the height of the peak, hence $N_{F1} \approx 3.0$ and $N_{F2} \approx 2.6$. The maximum decay rate during the relaxation time can also be measured: $\gamma_{front1} \approx 9.9$ and $\gamma_{front2} \approx 4.6$ (see figure 7 for probe 2). Assuming that in this initial phase of the relaxation the decay rate γ_{front} is related to the e-folding length λ_F, $\lambda_F = c_F/\gamma_{front}$, one can then estimate the particle content of the density pulse $\mathcal{N}/N_0 = (N_F/N_0 - 1)\lambda_F$. This estimate yields $\mathcal{N}_1/N_0 = 0.35$ and $\mathcal{N}_2/N_0 = 0.56$. The initial density burst is such that $\mathcal{N}/N_0 = 0.5$. Therefore, the particle conservation is approximately satisfied within a 10% error bar when considering data from probe 2, while data from probe 1, recorded prior to the triangular phase, is not properly taken into account by the proposed estimate. A proper integration of the particle content shows that the difference between probe 1 and 2 is less than 5%. One can then estimate the distance $\ell_{0,1}$ between the origin of the burst, located at $z = 0$, and probe 1. Using Eq.(9), and given $\ell_{1,2}$, one obtains:

$$\ell_{0,1} = \frac{1}{2}\Big(\ell_{1,2} + \frac{\mathcal{N}_1}{N_0}\mathcal{V}(N_{F1}/N_0) - \frac{\mathcal{N}_2}{N_0}\mathcal{V}(N_{F2}/N_0)\Big) \tag{12}$$

Using the data from probe 1 and 2 and the known function $\mathcal{V}$, one then finds that $\ell_{0,1} \approx 0.12$, corresponding to a 20% error with respect to the exact value 0.1 set in the simulation. As a consequence, one finds that the distance between probe 2 and the origin of the burst is $\ell_{2,0} \approx 0.48$ instead of 0.5. Using the data for probe 2 one can measure $N_{F0} \approx 3.43$ and using the relation Eq.(3) the density of the burst at $t = 0$ is found to be $N_{b2}/N_0 \approx 12.7$ instead of $N_b/N_0 = 10$. The error is comparable to that on the origin of the burst. Combining the latter estimate of the density of the burst and the estimate of the particle content of the burst, $\mathcal{N}_2/N_0 = 0.56$, one finds an estimate of the extent at $t = 0$, $z_{b2} \approx 0.044$ to be compared to $z_b = 0.05$. The study performed in this section, using numerical computation with rather

poor resolution, shows that it is possible to capture key features of the cross-field transport events when analyzing the imprint of such events on distant probes connected in the parallel direction. In the present framework it has been possible to estimate the origin of the burst, its density and extent in the parallel direction. Such information is of highest importance to assess the properties of the cross-field event, in particular, the strongly ballooned feature, estimated here by $\ell_{0,1}$, and the actual fraction of the filaments that are transported and determined by $2z_b$. Furthermore, the density of the cross-field burst can also be estimated, i.e N_b/N_0 in the present analysis.

IV. DISCUSSION AND CONCLUSION

The presented analytical work and the numerical modeling provide a comprehensive description of the parallel expansion of a density burst. The isothermal plasma is described by its density and parallel Mach number and is assumed quasi-neutral. The initial condition is an over-dense region with a finite parallel extent and a step shape. Two fronts detach from the initial density step and propagate with a supersonic velocity in the co and counter magnetic field directions. After a short transient, the fronts become independent and the density bursts exhibit a triangular shape. Using measurement of the signal at two different locations, we have been able to estimate the origin, the extent and the magnitude of the initial density step. The shape of the recorded density pulse leads to the characteristic ELM shape. The present work could provide a guideline to analyze the ELM shapes as a signature of the distance over which the parallel pulses have propagated. The front velocity scales like the sound velocity in agreement with measurements reported for the ELM propagation.

---

[1] Chiavassa G. et al. in preparation

[2] Landau L., Lifchitz E., *Mécanique des fluides*, MIR editions, Moscow 1971, p. 472.

[3] Fedorczak N. et al., *19th PSI conference, San Diego, May 2010.*

[4] Kirk A. et al., *Journal of Physics: Conference Series 123, 2008.*

[5] Oyama N. et al., *Nucl. Fusion 44, 2004.*

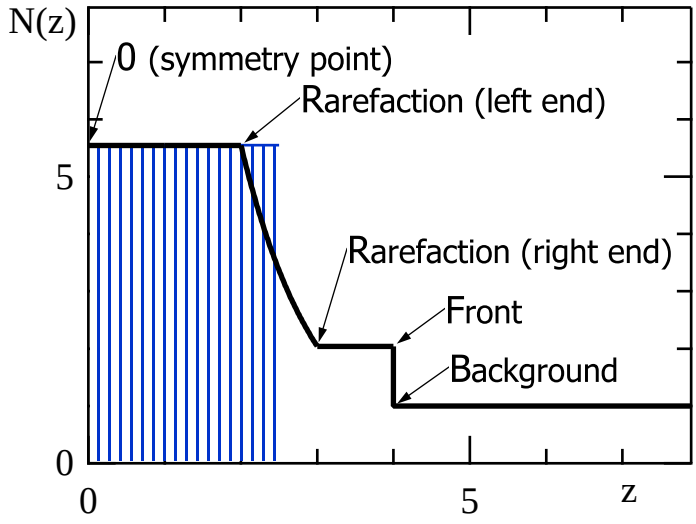

FIG. 1: Sketch of the density pulse, here extending from the symmetry point 0 to the point where the background conditions are recovered, the dashed area corresponds to the initial density burst

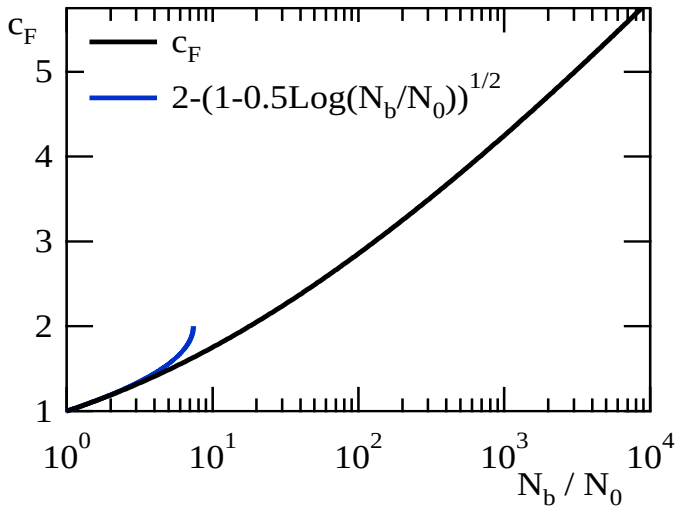

FIG. 2: Front velocity c_F as a function of the initial density step N_b/N_0 of the density burst, the blue curve is the approximate value for small density bursts in the range of turbulent transport

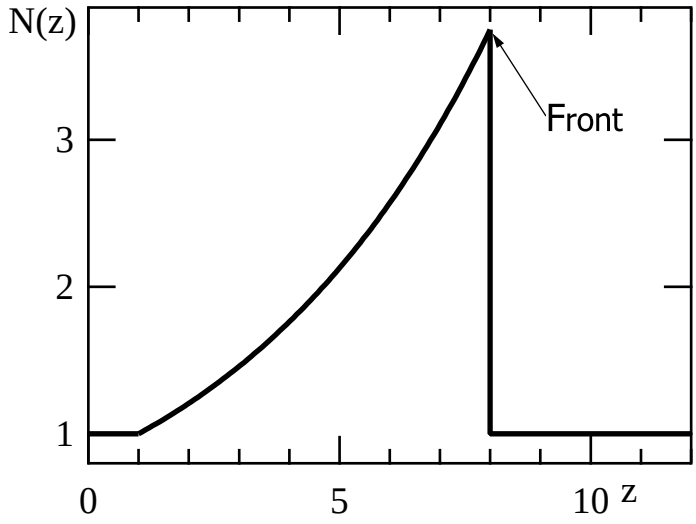

FIG. 3: Triangular wave form of $Log(N)$ of the density burst in the non-monotonic phase of the expansion

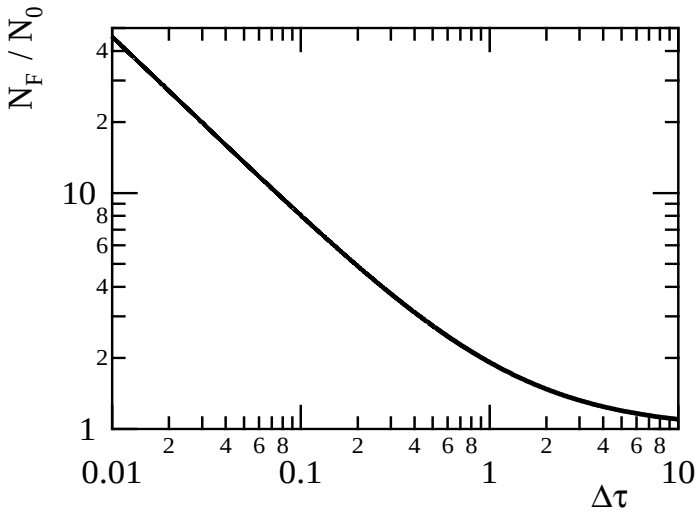

FIG. 4: Relaxation of the density at the front location with time

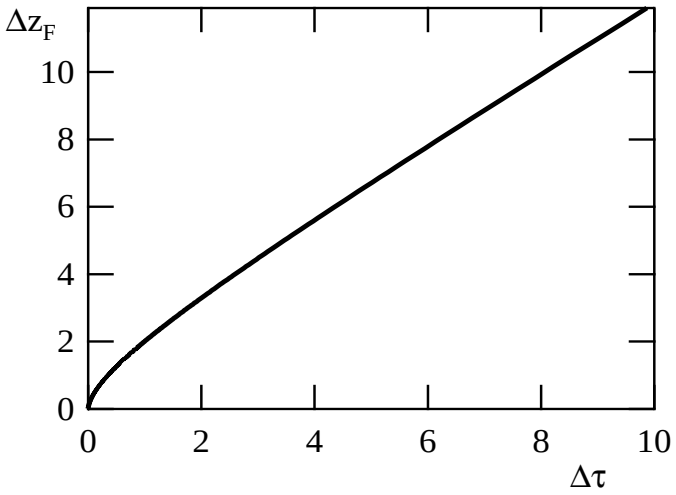

FIG. 5: Evolution of the triangular front location

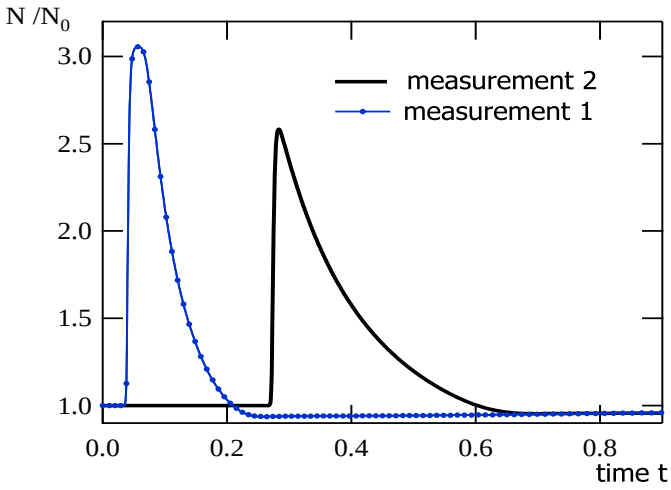

FIG. 6: Time traces of the density recorded at two measurement points.

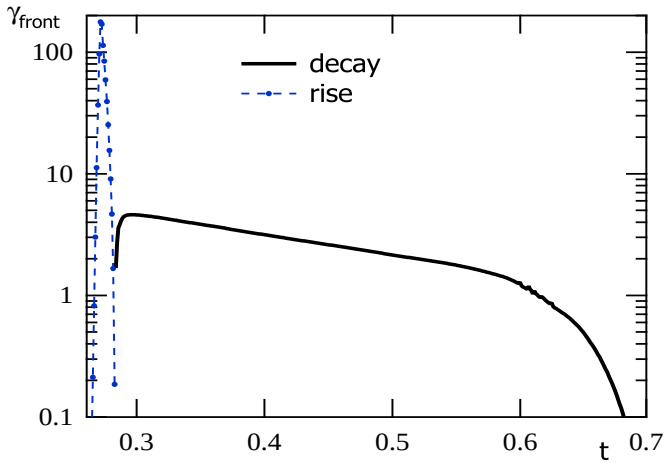

FIG. 7: Relaxation time of the density pulse for probe 2, blue curve rise time, black curve, decay time.